Energy Budget of Nonlinear Internal Waves near Dongsha

Ren-Chieh Lien
Applied Physics Laboratory
University of Washington
Seattle, Washington 98105
phone: (206) 685-1079 fax: (206) 543-6785 email: lien@apl.washington.edu

Eric A. D'Asaro
Applied Physics Laboratory
University of Washington
Seattle, Washington 98105
phone: (206) 685-2982 fax: (206) 543-6785 email: dasaro@apl.washington.edu

Award Number: N00014-05-1-0284

LONG-TERM GOALS

Our long-term scientific goal is to understand the mechanisms by which mixing occurs in the ocean and thereby help develop improved parameterizations of mixing for ocean models. Mixing within the stratified ocean is our particular focus as the complex interplay of internal waves from a variety of sources and turbulence makes this a current locus of uncertainty. In this study, our broad focus is on the energy sources of nonlinear internal waves (NLIWs) in a complex environment of strong internal tides and abrupt topography (continental shelf and slope). We expect a rapid evolution of internal tides and NLIWs, and we aim to understand their dynamics, energy cascade, and role in mixing.

OBJECTIVES

The primary objectives of the present project are 1) to identify the generation site and understand the generation mechanism of NLIWs, 2) to understand the evolution of NLIWs interacting with abrupt topography, 3) to quantify the energy budget and energy cascade from internal tides to NLIWs, and 4) to quantify the seasonal variation of the energy of NLIWs near Dongsha Island in the northern South China Sea (SCS). Our particular interest is to understand the energy cascade from barotropic tides, internal tides, NLIWs, to turbulence mixing in the northern SCS, and to understand the evolution of NLIWs interacting with the shoaling continental slope.

APPROACH

Our approach is to take direct observations of NLIWs near Dongsha Island where most of NLIW activities are captured in satellite images. In April-May 2005, we conducted a two-week observational experiment near Dongsha. Large-amplitude NLIWs, greater than 150 m, and strong turbulence mixing were observed by the Lagrangian float and shipboard sensors including ADCP, CTD, EK500, and X-band marine radar. Combined remote sensing and in-situ measurements provided detailed properties of large-amplitude NLIWs. In June 2006, an array of ADCP moorings was deployed along the prevailing path of NLIWs near Dongsha. Long-term observations of NLIWs will be obtained allowing us to (1) quantify the seasonal variation of NLIW energy, (2) map the geographical distribution, (3) better

Report Documentation Page

Form Approved
OMB No. 0704-0188

1. REPORT DATE	2. REPORT TYPE	3. DATES COVERED
30 SEP 2006		**00-00-2006 to 00-00-2006**

4. TITLE AND SUBTITLE	5a. CONTRACT NUMBER
Energy Budget of Nonlinear Internal Waves near Dongsha	5b. GRANT NUMBER
	5c. PROGRAM ELEMENT NUMBER
6. AUTHOR(S)	5d. PROJECT NUMBER
	5e. TASK NUMBER
	5f. WORK UNIT NUMBER
7. PERFORMING ORGANIZATION NAME(S) AND ADDRESS(ES) **University of Washington,Applied Physics Laboratory,1013 N.E. 40th St.,Seattle,WA,98105**	8. PERFORMING ORGANIZATION REPORT NUMBER
9. SPONSORING/MONITORING AGENCY NAME(S) AND ADDRESS(ES)	10. SPONSOR/MONITOR'S ACRONYM(S)
	11. SPONSOR/MONITOR'S REPORT NUMBER(S)

12. DISTRIBUTION/AVAILABILITY STATEMENT
Approved for public release; distribution unlimited

13. SUPPLEMENTARY NOTES

14. ABSTRACT

15. SUBJECT TERMS

16. SECURITY CLASSIFICATION OF:			17. LIMITATION OF ABSTRACT	18. NUMBER OF PAGES	19a. NAME OF RESPONSIBLE PERSON
a. REPORT **unclassified**	b. ABSTRACT **unclassified**	c. THIS PAGE **unclassified**	**Same as Report (SAR)**	**10**	

understand the dynamics of NLIW evolution over the shoaling topography, and (4) assess the model prediction skill of NLIWs.

WORK COMPLETED

A set of mooring ADCP data provided by Dr. David Tang of National Taiwan University was analyzed and results were published (Lien et al., 2005 and Chang et al., 2006). These ADCP measurements showed strong and highly predictable NLIWs on the continental slope and plateau in the vicinity of Dongsha Island. Strong energy flux divergence of NLIWs and internal tides are found across the Dongsha plateau.

Measurements taken in April 18-May 1 of 2005 are analyzed. Dr. Sue Moore, the whale expert at APL, was attracted to our video capture of a school of pilot whales in the NLIWs. A paper is to be published in Marine Mammal Science (Moore and Lien, 2006). We focus our analysis on describing 1) the rapid evolution of NLIWs on the shoaling continental slope, and 2) the surface signature induced by NLIWs. Results of these analyses were presented in the 2006 Ocean Sciences Meeting held in Honolulu and will be described in the next section.

A set of three bottom-mounted Long Ranger ADCPs were deployed in June 2006. These moorings are scheduled to take more than one year of measurements of NLIWs. They will be serviced every 3-4 months for retrieving data, replacing batteries, and maintenance.

RESULTS

Energy Flux and Flux Divergence across the Dongsha Plateau

Three sets of ADCP measurements taken on the Dongsha plateau, on the shallow continental shelf, and on the steep continental slope in the northern SCS are analyzed (Chang et al., 2006). The data show strong divergences of energy and energy flux of NLIWs along and across waves' prevailing westward propagation path (Fig. 1). The NLIW energy flux is 8.5 kW m-1 on the plateau, only 0.25 kW m-1 on the continental shelf 220 km westward along the propagation path, and only 1 kW m-1 on the continental slope 120 km northward across the propagation path. Along the wave path on the plateau, the average energy flux divergence of NLIWs is ~0.04 W m-2, which corresponds to a dissipation rate of O(10-7 –10-6) W kg-1 for NLIWs. Combining these observations and model results, we conclude a scenario of NLIW energy flux in the SCS. NLIWs are generated east of the plateau, propagate predominantly westward across the plateau along a beam of ~100 km width that is centered at ~21oN, and dissipate nearly all their energy before reaching the continental shelf.

Properties of NLIWs on Shoaling Continental Slope

In April-May 2005, our measurements were taken mostly along 21ºN between 118 on the upper continental slope and 116.5ºE on Dongsha plateau of about 350-500-m depth (Fig. 2) using shipboard ADCP, CTD, EK500, marine Radar, XBT, and a Lagrangian float. The float measures internal waves and turbulence mixing.

The NLIW evolves rapidly as it propagates westward up the continental slope onto Dongsha plateau. On April 28, the details of the evolution were captured by shipboard observations and summarized in Fig. 3. The NLIW first appears as a single-depression wave with amplitude > 170m. Within two hours and in a distance of 10 km, a small wave is born trailing immediately behind the original wave, identified by marine radar measurements. The small wave propagates slower than the leading large wave, and is further separated from the leading wave as they propagate westward across Dongsha plateau.

The dynamics of this fission process is important for the energy evolution of NLIWs, but is yet not well known. A closer look of the velocity structure and the speed of NLIWs provides a hint of the evolution (Fig. 4). As the NLIW shoals, the wave speed decreases immediately responding to the local depth, whereas the maximum fluid velocity remains unchanged for a while. A trapped core is formed. Within the trapped core, *Ri* is smaller than ¼, and the dissipation rate of turbulence kinetic energy is O (10-5) W kg-1 observed by the Lagrangian float (Fig. 5). An overturning scale of 75 m is observed. More than 3.5 hours after the NLIW reduces its speed, the maximum horizontal velocity of the NLIW begins to decrease gradually, presumably as a result of the combined fission process and dissipation. About another 3 hrs later, the trapped core disappears (Fig. 4). The cartoon in Fig 6 illustrates the proposed scenario of the trapped core formation, fission, dissipation, and evolution of NLIW on the shoaling topography. The hypothesis needs to be further investigated by observations and model simulations.

Remote Sensing and Prediction of Properties of Nonlinear Internal Waves

We analyze the simultaneous set of marine radar, shipboard ADCP, CTD, and echo sounder observations of large-amplitude NLIWs in the SCS. Primary causes of strong surface scattering in radar observations are winds and NLIWs. In the absence of NLIWs, the wind speed is strongly correlated with the radar scattering intensity with a correlation coefficient of 0.87, but the correlation disappears when NLIWs are present. We analyze properties of NLIWs and radar surface scattering intensity during events of strong NLIWs and construct a composite structure of NLIWs and the corresponding surface scattering strength.

The average half width ($\lambda_{\eta/2}$) of NLIWs, i.e., the spatial scale of one half of the maximum amplitude of NLIWs, is 1.09 ± 0.2 km (Fig. 7). The average half width of the scattering intensity and strain rate is 0.57 ± 0.12 $\lambda_{\eta/2}$ (top panels in Fig. 7) and 0.46 ± 0.06 $\lambda_{\eta/2}$ (middle panels in Fig. 7), respectively. The strong surface scattering leads the maximum amplitude of NLIWs by 0.46 ± 0.11 $\lambda_{\eta/2}$. Surface scattering intensity measured by the radar looking from behind the NLIW (blue curves in the top panels) is 76% of that measured by the radar looking from ahead the NLIW (red curves in the top panels). In the divergence zone ($\frac{du}{dx}$ >0), the rear portion of NLIWs, surface scattering intensity observed by the radar is not significantly different from the background (Fig. 8). In the convergence zone ($\frac{du}{dx}$ <0), the front portion of NLIWs, the surface scattering intensity is positively proportional to the magnitude of the strain rate. A linear regression line fits reasonably well in -1.8x10-3 s-1 < $\frac{du}{dx}$ < 0 s-1 with a correlation coefficient -0.93 (red curves). Over the entire strain rate observed, an arctangent model fits better (blue curves). Our results conclude that strain rates, horizontal scales, and positions of NLIWs are predictable

by remote sensing observations. The application of these results on satellite derived surface signatures of NLIWs is practical.

IMPACT/APPLICATION

Our analysis concludes that NLIWs evolve rapidly across the upper flank of the continental slope and the Dongsha plateau via complicate processes, e.g., the formation of trapped cores, and the development of wave train. These processes are responsible for the strong dissipation of NLIWs in SCS. Our analysis of combined remote sensing and in-situ measurements yields a model for predicting NLIW properties applicable to satellite observations. Further long-term observations of NLIWs in the vicinity of Dongsha plateau are in progress and will provide a better prediction of NLIWs in SCS.

REFERENCES

Chang, M.-H., R.-C. Lien, T. Y. Tang, E. A. D'Asaro, and Y. J. Yang, Energy flux of nonlinear internal waves in northern South China Sea, *Geophys. Res. Lett*., 33, L03607, doi:10.1029/2005GL025196, 2006.

Chang, M.-H., R.-C. Lien, T. Y. Tang, Y. J. Yang, and J. Wang, Surface signatures of nonlinear internal waves in South China Sea: properties and predictions, to be submitted to *J. Geophys. Res*., 2006.

Lien, R.-C., T. Y. Tang, M. H. Chang, E. A. D'Asaro, Energy of nonlinear internal waves in the South China Sea, *Geophys. Res*. *Lett.*, **32**, L05615, doi:10.1029/2004GL022012, 2005.

Zhao, Z., V. Klemas, Q. Zheng, and X.-H. Yang, Remote sensing evidence for baroclinic tide origin of internal solitary waves in the northeastern South China Sea, *Geophys. Res. Lett.*, **31**, L06302, doi:10,1029/2003GL019077, 2004.

PUBLICATIONS

Lien, R.-C., T. Y. Tang, M. H. Chang, E. A. D'Asaro, Energy of nonlinear internal waves in the South China Sea, *Geophys. Res*. *Lett.*, **32**, L05615, doi:10.1029/2004GL022012, 2005.

Chang, M.-H., R.-C. Lien, T. Y. Tang, E. A. D'Asaro, and Y. J. Yang, Energy flux of nonlinear internal waves in northern South China Sea, *Geophys. Res. Lett.*, **33**, L03607, doi:10.1029/2005GL025196, 2006.

Moore, S. E., and R.-C. Lien, Pilot whales follow internal solitary waves in the South China Sea, *Mar. Mamm. Sci.*, in press, 2006.

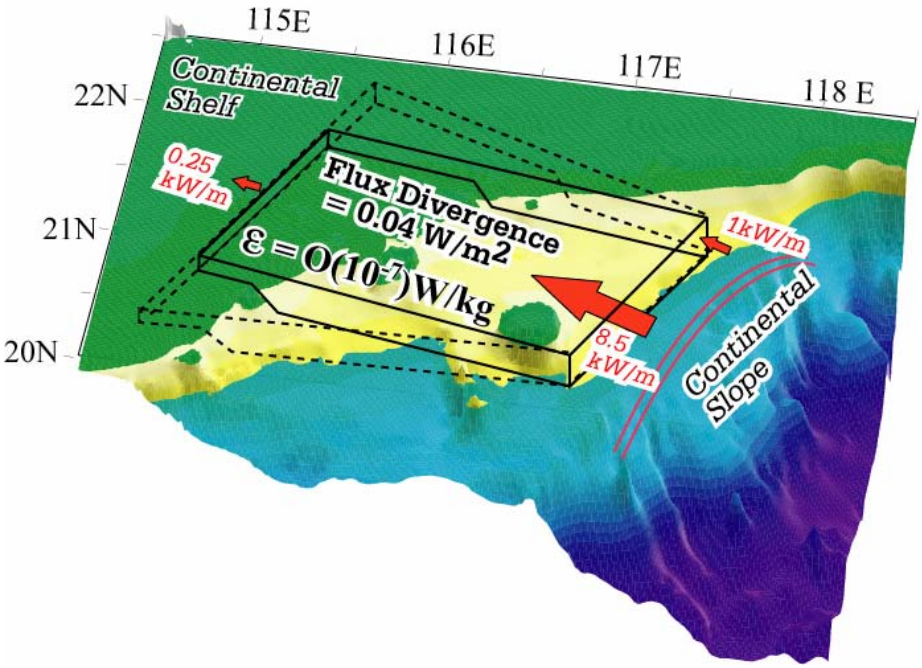

Figure 1: Flux divergence of NLIWs on Dongsha plateau. The average dissipation rate is calculated as $\varepsilon = \frac{\Delta F}{\Delta s}$ ***, where*** ΔF ***is the difference between the vertically integrated energy flux of NLIWs on the eastern edge of the Dongsha plateau, 8.5 kW m-1, and that on the continental shelf, 0.25 kW m-1, and*** Δs ***is the distance between the two stations. The flux divergence is ~0.04 W m-2, corresponding to a dissipation rate of O(10-7) W kg-1 for NLIWs. The dashed-line and solid-line boxes illustrate the horizontal spreading of NLIWs energy.***

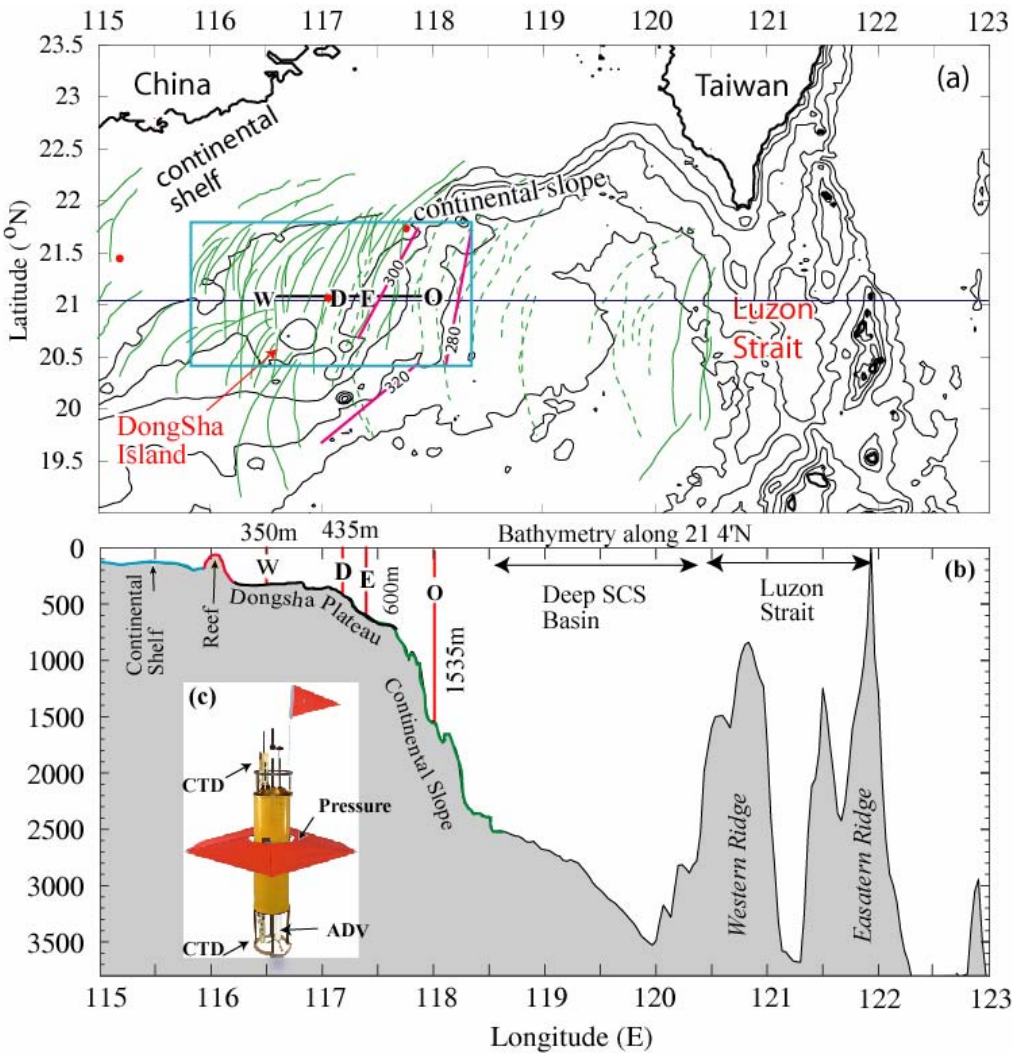

Figure 2: (a) Map of the northern South China Sea, and (b) bottom bathymetry along 21°4'N. In panel (a), green curves represent surface signatures of NLIWs identified in satellite images (Zhao et al., 2004), dashed for single-depression waves and solid for multiple wave packets. The blue box delineates the area where multiple wave packets are mostly found. Four primary stations in our April-May 2005 cruise are labeled as O, E, D and W. Shipboard and float measurements are taken along O-E-D-W. Three magenta curves illustrate isobaric orientations on the continental slope. In panel (b), two submarine ridges in the Luzon Strait are labeled. They are responsible for generating strong internal tides. Depths at four primary stations are also labeled. The inset (c) shows the Lagrangian float and sensors equipped on the float.

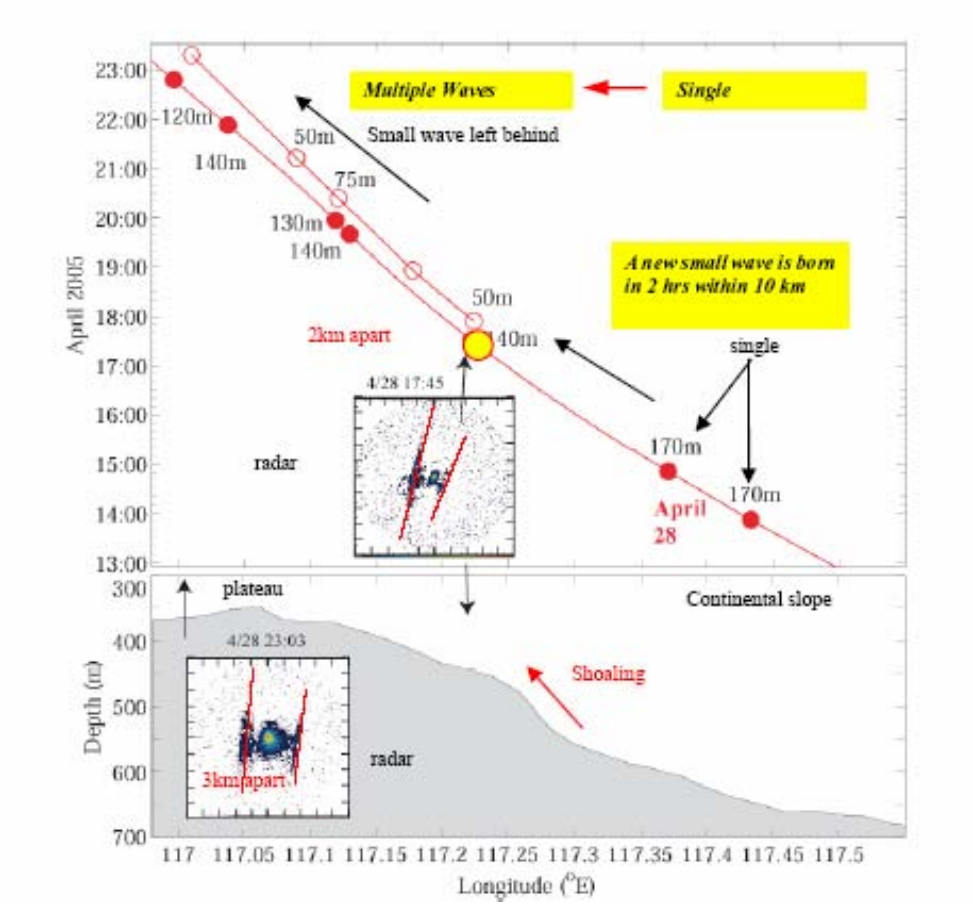

Figure 3: The top panel shows the evolution of NLIWs propagating westward on the shoaling continental slope captured by shipboard measurements in April 28, 2005. Solid dots represent the leading wave, and open circles are trailing wave. Amplitudes of NLIWs are labeled. The bottom panel shows the bottom topography. Two insets are illustrations of radar images taken at 1745 LT on the upper flank of the continental slope and at 2303LT on the plateau. Red lines on radar images indicate crests of NLIWs.

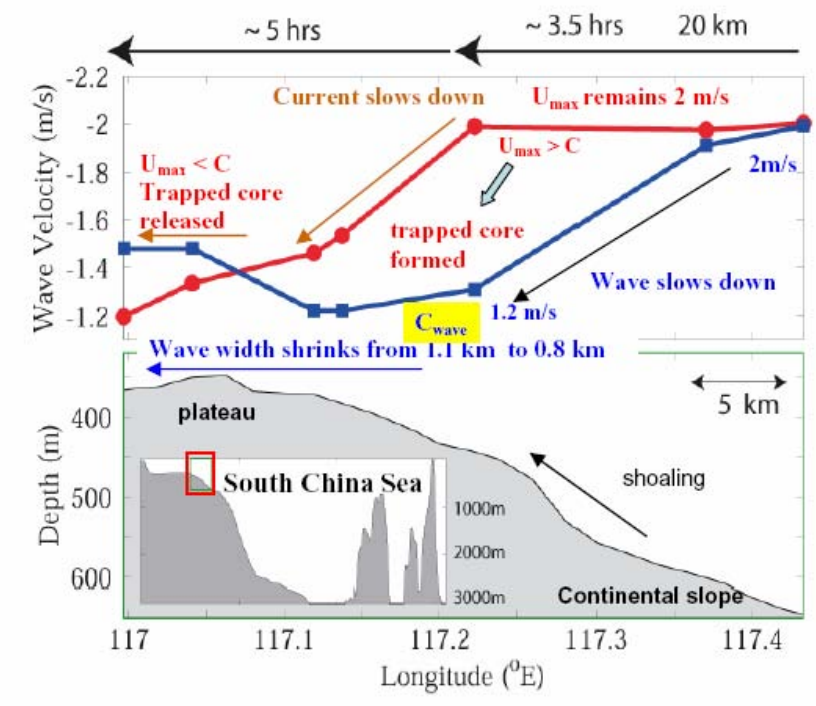

Figure 4: The top panel summarizes the variations of the maximum horizontal velocity (red curve) and the wave speed (blue curve) of a large-amplitude NLIW propagating westward on the shoaling continental slope. The bottom panel shows the bottom bathymetry. The red box in the inset delineates the location of our observations.

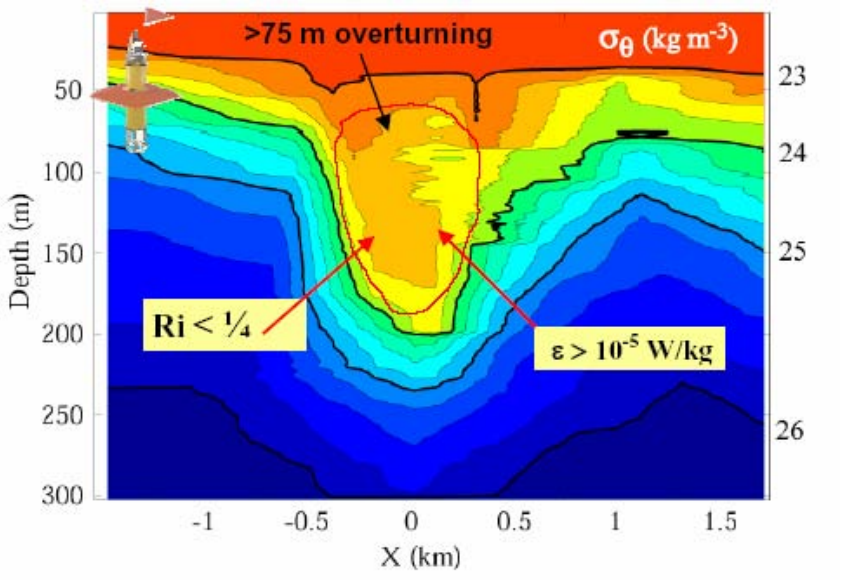

Figure 5: The density contour obtained by the shipboard CTD illustrates ~75-m overturn. The Richardson number and ε following the Lagrangian float are estimated. The red enclosure indicates the possible trapped core.

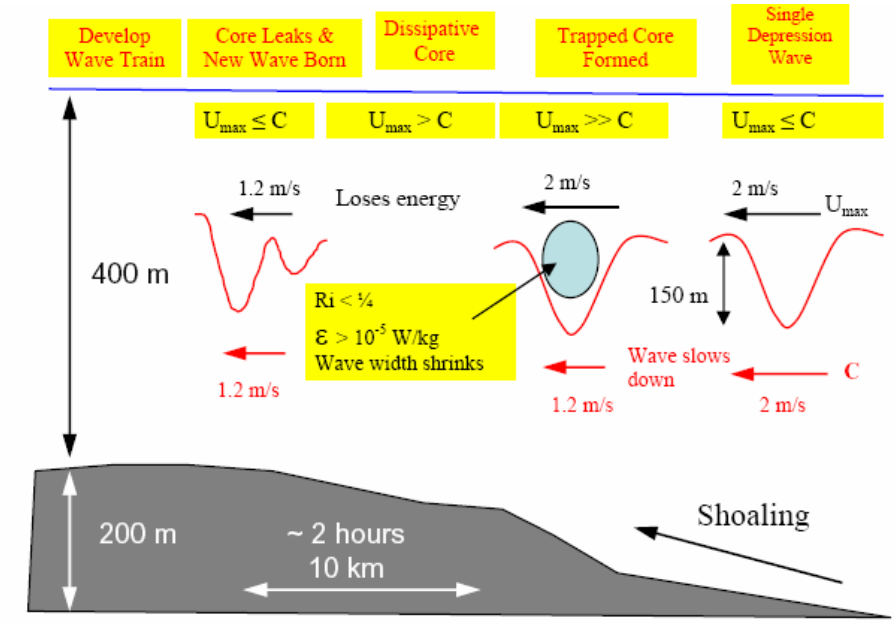

Figure 6: A summary cartoon illustrates the evolution of NLIWs on the shoaling continental slope across the Dongsha plateau.

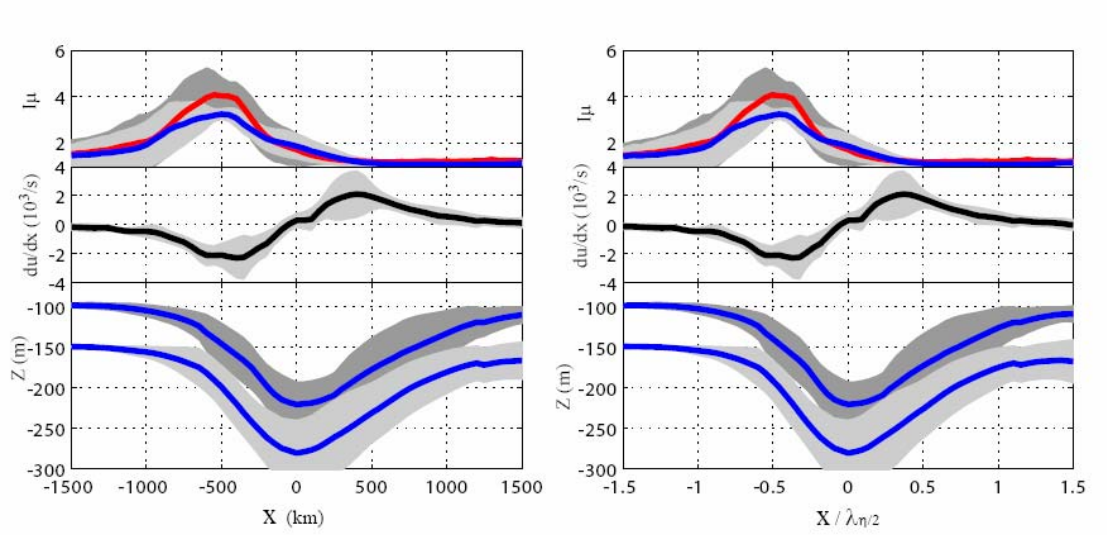

Figure 7: Spatial structures of the surface scattering intensity observed by the marine radar (top panels), the horizontal strain rate observed by the shipboard ADCP at 14-m depth (middle panel), and isopycnal displacements at equilibrium depths of 100 m and 150 m (bottom panels). The NLIW propagates toward the left of the page. These properties are averaged over all large-amplitude NLIWI events. The left panels show the actual spatial scale, where X is the horizontal scale in the propagating direction of NLIWs. In the right panels, X is normalized by the half-amplitude wave width of NLIWs. The surface scattering intensity depends on the position of the radar relative to the propagating direction of NLIWs. The intensity is stronger when the radar is ahead of the NLIW (red curves), and is weaker when the radar is behind the NLIW (blue curves). Gray shadings represent 95% confidence intervals.

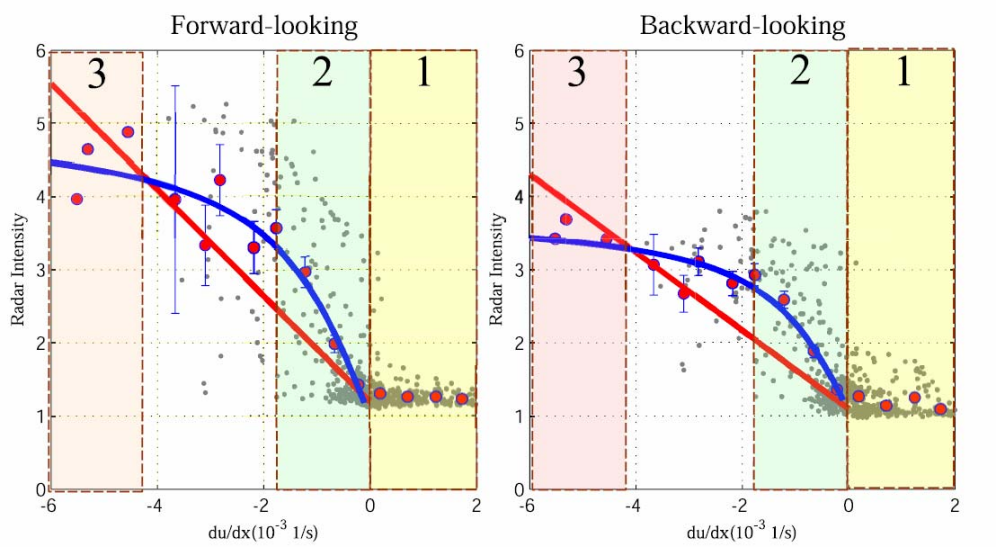

Figure 8: Scattering plots and model fits between surface scattering intensity observed by radar and the strain rate computed from shipboard ADCP measurements. The left panel shows observations (gray dots) when the radar is ahead of the propagating NLIWs. Red dots represent averages over constant grid interval, 0.005 s-1, of the strain rate. Vertical lines represent 95% error bars. Red and blue curves represent the linear and arctangent fits to observations (red dots). Three regions labeled as 1, 2, and 3 represent the divergence zone, the weak convergence zone, and the strong convergence zone. Symbols, curves, and labels in the right panel are the same as in the left panel, but radar observations are taken behind the propagating NLIWs.